



Using α -Fe₂O₃/SiO₂ as a heterogeneous Fenton catalyst for the removal of chlorophenol in aqueous environment: Thermodynamic and kinetic studies

A. Shokri¹ · M. Sanavi Fard²

Received: 23 March 2022 / Revised: 2 August 2022 / Accepted: 21 August 2022 / Published online: 7 September 2022

© The Author(s) under exclusive licence to Iranian Society of Environmentalists (IRSEN) and Science and Research Branch, Islamic Azad University 2022

Abstract

Wastewater containing chlorophenol (CP) can potentially pose a considerable hazard to human beings and the environment, which demands an imperative and effective treatment process before releasing to the environment. The current study focused on the optimization of the heterogeneous Fenton process using Fe₂O₃/SiO₂ as a catalyst for the removal of CP from wastewater by full factorial experimental design. The catalyst was prepared by the solid-state dispersion (SSD) method and characterized by XRD, FTIR, and SEM techniques. The mechanism of the heterogeneous Fenton process by α -Fe₂O₃/SiO₂ catalyst as a source of ferrous ions was described. The effect of three major parameters including time, the mass ratio of H₂O₂ to chlorophenol, and catalyst dosage besides their interactions was studied. The optimum conditions for each critical factor were as follows: time = 30 min, a mass ratio of H₂O₂ to CP = 4.96, catalyst dosage = 4.5 g/l. The maximum efficiency in the experimental and predicted CP removal was 98.9 and 97.71%, respectively. The kinetic study exhibited that the degradation of CP followed a pseudo-second-order reaction kinetic model with rate constants in a range of 0.00421 to 0.00507 (L mg⁻¹ min⁻¹). The standard Gibbs free energies (ΔG°), standard reaction enthalpies (ΔH°), activation energies (E_a), standard entropies (ΔS°) were found in a range of -4.343 to -5.396 kJ mol⁻¹, 5.95 kJ mol⁻¹, 5.05 kJ mol⁻¹, and 35.13 J mol⁻¹ k⁻¹, respectively. Thus, it can be concluding that heterogeneous Fenton is an effective and reliable technology in the treatment of CP in an aqueous environment.

Keywords Heterogeneous Fenton process · Chlorophenol removal · Thermodynamic and kinetic studies · Full factorial design · α -Fe₂O₃/SiO₂ catalyst

Introduction

Detoxifying process of various wastewater sources is highly problematic because of the presence of highly toxic, complicated, and various organic contaminants that are recalcitrant to traditional treatment methods (Pervez et al. 2020; Mushtaq et al. 2020). As a result, effective removal of different types of perilous organic pollutants from water and wastewater is a crucial challenge in environmental research

areas which pose significant threats on all fronts. Among those contaminants, phenolic compounds have been detected as potentially harmful contaminants and can cause harmful effects on various biological processes (Pervez et al. 2020). Phenols and their chlorinated compounds are toxic to both aquatic communities and human health. Because of the bio-refractory nature of phenolic-based wastes, they cannot be typically treated by conventional processes.

Moreover, chlorophenol compounds are quickly absorbed when consumed by the respiration or oral system (Matafonova et al. 2011). Different industries including coal conversion, pharmaceutical, textile, coal mining, building materials, pesticides, artificial rubber, chemicals, paper, plastics, automobile, resin manufacturing, and oil industries are the main origins of phenolic compounds in the environment. As wood preservatives, chlorophenols are extensively utilized, and for antiseptic production in industrial activities, usually 4-Chlorophenol is utilized (Shokri 2020). Based on the

Editorial responsibility: Lifeng Yin.

✉ A. Shokri
aref.shokri3@gmail.com

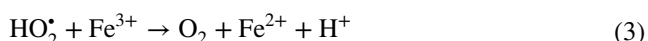
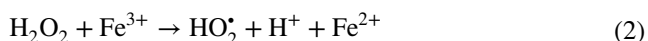
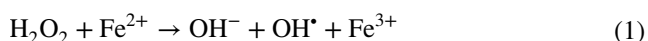
¹ Jundi-Shapur Research Institute, Jundi-Shapur University of Technology, Dezful, Iran

² Department of Chemical Engineering, Tafresh University, Tafresh, Iran



WHO (World Health Organization), the acceptable concentration of chlorophenols in potable water is 1 mg L^{-1} (Hadi et al. 2020).

Recently, various methods have been utilized to remove chlorophenol from an aqueous environment, including radiation-induced degradation (Rauf and Ashraf 2009), catalytic wet oxidation (Rocha et al. 2021), electrochemical oxidation (Clematis and Panizza 2021), chemical reduction treatment by zero-valent iron (Li et al. 2021a), adsorption (Li et al. 2021b) and solvent extraction. Moreover, processes like hypochlorite oxidation and ozone oxidation are to some extent efficient for pollutant degradation however are not desirable because of their intrinsic disadvantage associated with cost, performance, and formation of wastes as side-products (Ye et al. 2020; Hou et al. 2020). Recently, the advanced oxidation processes (AOPs) have absorbed significant attention because of their substantial ability to the degradation of various refractory organic contaminants. In comparison with physical and biological methods, AOPs are highly advantageous since they degrade different organic materials with high toxicity, whereas the biological processes are time-intensive and the physical methods generate secondary waste. Their considerable efficiency heavily depends on the non-selective and powerful feature of OH^\bullet generation. Between different methods of AOPs, the oxidation by Fenton's reagent has demonstrated significant promise due to its efficiency in the degradation of a broad range of toxic organic contaminants (Feng et al. 2019). Because of the less toxic nature of reagents, simplicity, high efficiency, and economic feasibility of the Fenton process, it has been broadly utilized for contaminant degradation in wastewater (Xu and Wang 2012). The Fenton process utilizes ferrous and H_2O_2 for the production of powerful OH^\bullet in an aqueous environment (Pervez et al. 2019) which has the ability to degrade many organic pollutants. By the further reaction of Fe^{3+} with H_2O_2 , the utilized Fe^{2+} in the Fenton process is generated again (Eqs.1–3).



Despite the advantages of Fenton-based treatment processes (Karimi et al. 2012; Chen et al. 2017), homogeneous Fenton reactions including Fe^{2+} and H_2O_2 have several major drawbacks such as the requirement for maintaining extreme acidic conditions (the optimal pH is around 3), formation of a remarkable quantity of iron sludge and non-reusable reagent which is cost-prohibitive and ineffective (Nidheesh

et al. 2013; Morshed et al. 2020). Hence, numerous research work has been dedicated to enhancing the treatment performance of the Fenton process besides reducing the generation of contaminants as side products (Zhang et al. 2019). In the view of the current scenario, instead of using ferrous, the heterogeneous Fenton process has advent as a promising technology to overcome the aforesaid shortcomings by the application of recyclable solid catalysts (Nidheesh 2015; He et al. 2016). Even though significant research has mainly focused on designing quite effective heterogeneous Fenton catalysts, still several unresolved questions considering the principles of heterogeneous catalysis are evident (Sun et al. 2018, 2020). Besides the properties of reactive oxidants generated in the heterogeneous Fenton process, still there is continuous controversy about the oxidation fundamentals of target compounds by the produced oxidants. Fundamentally, the improved catalytic efficiency of several efficient Fenton solid catalysts has been determined, to promote exposure of adsorbed pollutants to oxidants generated at or in the proximity of surface sites (Gonzalez-Olmos et al. 2013; He et al. 2020). Contrarily, based on various investigations, adsorbed organics on the surface of iron oxide catalysts were not oxidized and thus suggested that surface-produced hydroxyl radicals mainly oxidize organic compounds in the aqueous environment (Liang et al. 2012). Despite the broad exploration regarding the heterogeneous Fenton reaction, whether the degradation of pollutants occurs in the interfacial boundary layer, solution, or on the catalyst surface or their integration, is unresolved (Waite et al. 2021).

In the heterogeneous Fenton process, not only metal ions can be easily separated from the solution but also a great quantity of iron or any metal ion that is utilized as a catalyst remains in the solid phase. To decrease the quenching of OH^\bullet , the quantity of Fe^{2+} must be maintained at small levels. In this vein, the heterogeneous Fenton process has been developed by researchers (Waite et al. 2021). The heterogeneous Fenton process has several benefits like the absence of side-products as contaminants, catalyst reusability, and broader operational pH window.

The full factorial design (FFD) has gained significant focus as a series of statistical and mathematical methods appropriate for exploring the effects of several independent parameters of the experiment. In comparison with OFAT (one factor at a time) approach, FFD has different advantages like needing lower experiments, reduced time of the experiment, cost-effective, and enough adequacy in the prediction of the response. To our best knowledge, there is no research work considering the optimization and statistical modeling of heterogeneous Fenton for the removal of chlorophenol utilizing $\alpha\text{-Fe}_2\text{O}_3/\text{SiO}_2$ catalyst by full factorial design of experiment. Hence, as a novel research work, current research utilizes FFD with 27 runs to optimize the elimination of chlorophenol



using the heterogeneous Fenton process. The effects of time, the mass ratio of H_2O_2 to chlorophenol, and the amount of catalyst as the critical factors on the percentage of chlorophenol removal as a response were studied by Design-Expert software. The capability of the system for the removal of chlorophenol at the optimal condition was explored. The kinetic and thermodynamic studies were performed, and the ΔH° , ΔG° , E_a , and ΔS° were obtained. Moreover, the preparation of $\alpha\text{-Fe}_2\text{O}_3/\text{SiO}_2$ catalysts besides its characterization and the process mechanism are discussed.

Materials and methods

Materials and apparatuses

4-Chlorophenol with a purity of higher than 98% was supplied from TCI (Shanghai, China) and utilized without additional purification. All chemicals used, such as iron oxides, ethanol, and so on, for the synthesizing catalyst were supplied from Merck Company. The chemical properties of 4-Chlorophenol are presented in Table 1.

BELSORP-mini II, DX27-mini, Perkin-Elmer (Spectrum Two, model), and Philips XL-30, devices were used as BET surface area analyzer, X-ray diffractometer (XRD), and Fourier transform infrared (FTIR) spectrometer, and scanning electron microscope (SEM), respectively. Moreover, for taking UV/Vis absorption spectra, Agilent 8453 spectrophotometer was utilized.

Catalyst preparation and characteristics

Synthesizing of iron hydroxide ($\text{Fe}(\text{OH})_2$)

To prepare iron hydroxide as a precursor of iron oxide, according to Bharathi et al. (Bharathi et al. 2010), 100 ml of urea (1 M) was slowly added to 100 ml of iron chloride (0.25 M). The resulting solution was then exposed to reflux conditions for 12 h at a temperature of 95–90 °C. The reflux precipitate was washed with deionized water several times to remove the entire unreacted materials. The washed

precipitate, which was $\text{Fe}(\text{OH})_2$, was completely dried at 70 °C.

Preparation of $\alpha\text{-Fe}_2\text{O}_3/\text{SiO}_2$ catalyst

The $\alpha\text{-Fe}_2\text{O}_3/\text{SiO}_2$ has been utilized as a catalyst for the heterogeneous Fenton reaction and the concentration of the catalyst has meant its value on the base. Based on the report of Nikazar et al., $\alpha\text{-Fe}_2\text{O}_3/\text{SiO}_2$ catalyst was prepared by the solid-state dispersion (SSD) method (Nikazar et al. 2008). For this purpose, firstly, the produced iron hydroxide 1:3 was mixed with silica (support catalyst) for one hour with a small quantity of ethanol. The addition of ethanol was performed to such an extent that the mixture takes a mud-like state and making the mixing operation easier. The resulting mixture was dried at 70 °C and then exposed to 300 °C for one hour to not only the iron hydroxide particles supported on the silica surface become iron oxide but also become thermally stabilized on the surface of silica (Bharathi et al. 2010).

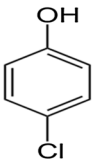
Characterization of the supported catalysts

The SEM images of the SiO_2 support catalyst and the $\alpha\text{-Fe}_2\text{O}_3/\text{SiO}_2$ catalyst are demonstrated in Fig. 1a, b, respectively. Figure 1b shows well that $\alpha\text{-Fe}_2\text{O}_3$ particles are supported spherically and uniformly distributed on the surface of silica. This image also shows that in some parts of the silica surface, more $\alpha\text{-Fe}_2\text{O}_3$ particles have accumulated, which can be due to two reasons: first, the morphology of the silica surface, second, the adhesion of fine iron oxide particles to each other and their accumulation in one special area.

Figure 2 (above one) shows the FTIR spectrum of the SiO_2 support catalyst, in which the characteristic peaks of the Si–O–Si and Si–H vibrations are shown. The appearance of the characteristic Fe–O peak in this spectrum is due to the small amount of iron oxide in the mineral (natural) silica used in this study. The FTIR spectrum of the $\alpha\text{-Fe}_2\text{O}_3/\text{SiO}_2$ catalyst is shown in Fig. 2 (below one). The increase in peak intensity characteristic of Fe–O vibration indicates an increase in the amount of iron oxide in the material, which means the stabilization of $\alpha\text{-Fe}_2\text{O}_3$ particles on the SiO_2 surface and confirms the results of SEM images. Characteristic peaks of $\alpha\text{-Fe}_2\text{O}_3$ are evident which are in harmony with the results of Bharathi et al. (Bharathi et al. 2010). Such characteristic peaks, which are associated with bending modes and stretching of Fe–O and OH in FeOOH , sometimes overlap with specific peaks of SiO_2 .

The above and down curves in Fig. 3 show the XRD patterns of the base of the SiO_2 catalyst and the $\alpha\text{-Fe}_2\text{O}_3/\text{SiO}_2$ catalyst, respectively. As can be seen, in the $\alpha\text{-Fe}_2\text{O}_3/\text{SiO}_2$ pattern, all characteristic SiO_2 peaks appear, only slightly reduced in intensity, which means that during the supporting process, the supported catalyst is not structurally

Table 1 Chemical properties of 4-Chlorophenol

Pollutant	Molecular structure	λ_{max} (nm)	Molecular Mass (g/mol)
4-Chlorophenol ($\text{C}_6\text{H}_4\text{ClOH}$)		225	128.56



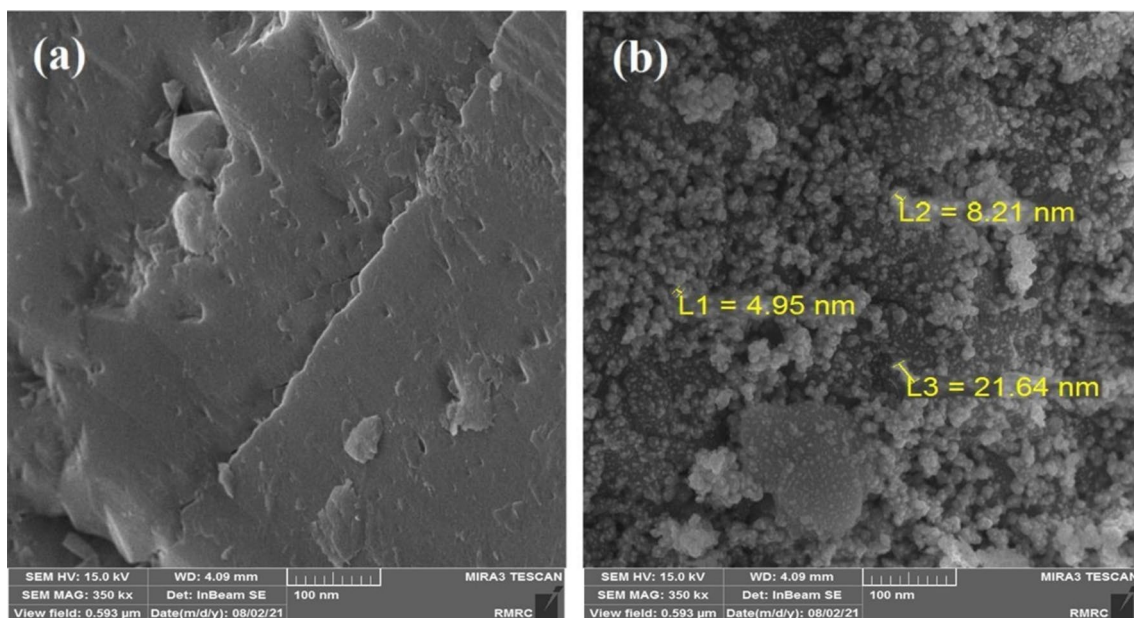
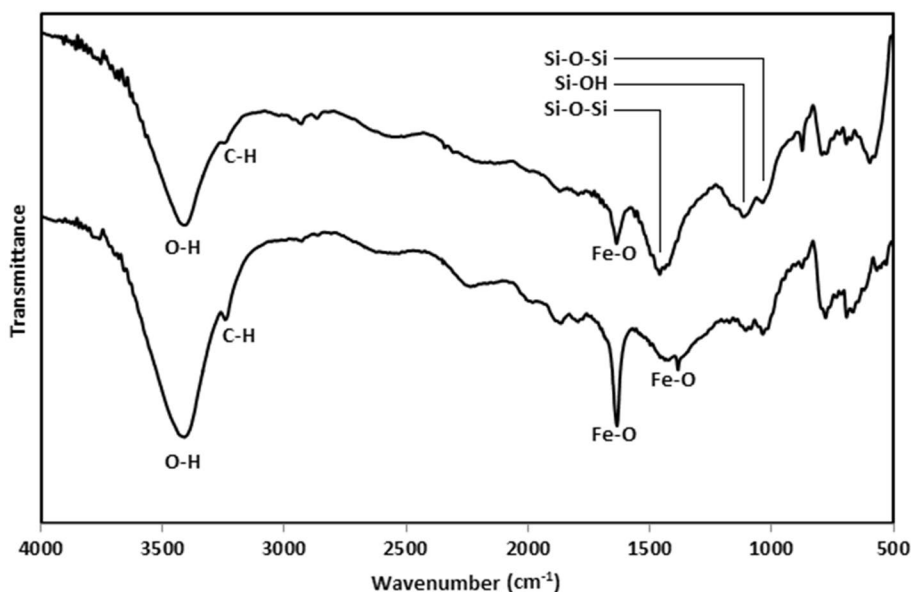


Fig. 1 SEM images related to **a** SiO_2 catalyst support and **b** $\alpha\text{-Fe}_2\text{O}_3/\text{SiO}_2$ catalyst

Fig. 2 FTIR spectra related to catalyst support (top) and $\alpha\text{-Fe}_2\text{O}_3/\text{SiO}_2$ catalyst (down)



or chemically changed and only its surface is covered with iron oxide. The reason for reducing the intensity of the SiO_2 peaks is due to the coating of the SiO_2 surface with iron oxide. The emergence of $\alpha\text{-Fe}_2\text{O}_3$ specific peaks in the low XRD pattern, which is in good harmony with the results of Bharathi et al. (Bharathi et al. 2010), is indicative of the successful synthesis and stabilization of iron oxide. The XRD pattern of $\alpha\text{-Fe}_2\text{O}_3/\text{SiO}_2$ using Warren–Averbach theory (Barka and Assabane 2008) and calculating the device errors showed that the average crystal size of this catalyst is about 12 nm.

Procedure and experimental design

The experimental works were performed in a glass photoreactor with a one-liter capacity and prepared to utilize a sampling system (Fig. 4). Its UV irradiation was a 15 W Philips Company in Holland vertically located at the center of the reactor and was turned off in all experiments. The experimental setup provided a jacket of water with an external flow adapted using a thermostat to control the temperature. In order to control temperature, the water bath, from the Korean Company, the BW-05G model was used.



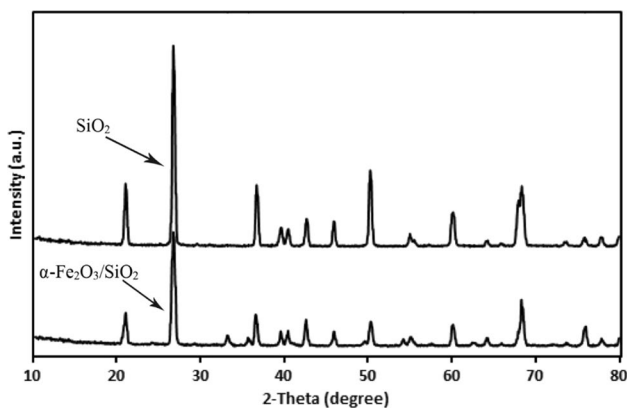


Fig. 3 XRD patterns related to catalyst support (top) and $\alpha\text{-Fe}_2\text{O}_3/\text{SiO}_2$ catalyst (down)

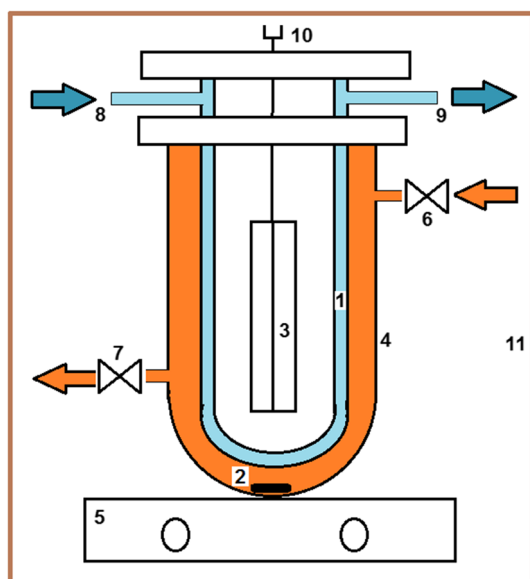


Fig. 4 Schematic figure of the utilized reactor in the experiment. (1) Quartz immersion well, (2) Magnetic stirrer bar, (3) UV lamp, (4) Glass reactor, (5) Magnetic stirrer, (6) Loading valve, (7) Unloading valve & Sampling point, (8) Cooling water source, (9) Cooling water return, (10) Electric connection, (11) Dark Box

A synthetic effluent containing 75 mg L^{-1} of chlorophenol was used for the conduction of the experimental design and it was conveyed into the reactor. To prevent the precipitation of iron ions in the reactor and create a homogenized environment the solution was stirred. The progress in the degradation of 4-Chlorophenol was examined by UV/Vis spectrophotometer at a maximum wavelength of 225 nm and confirmed by high-pressure liquid chromatography (HPLC). Our response was only the percentage of chlorophenol removal, which was measured at 225 nm (this peak was more accurate). The UV spectrum was taken from the

effluent during treatment. Based on the preliminary experiments, the differences between neutral and acidic pH were slight, therefore, the pH was fixed at 6 in all runs which was the real pH of synthetic wastewater containing 4-Chlorophenol. The catalyst was synthesized, and the iron was placed on silica. Under optimal conditions, 70% of the chemically required oxygen (COD) was removed, to be more specific, it was reduced from 300 to 90 mg L^{-1} . The increased conductivity of the effluent was also related to the produced chlorine and the extraction of iron ions from the catalyst tissue. Catalyst identification tests are evaluated in the following. The removal of chlorophenol is measured using the following equation (Eq. 4):

$$\text{Removal of CP}(\%) = \frac{[\text{CP}]_0 - [\text{CP}]}{[\text{CP}]_0} \times 100 \quad (4)$$

where $[\text{CP}]_0$ and $[\text{CP}]$ are the concentration of the 4-Chlorophenol at the beginning of the reaction and at the time t , respectively.

Experimental design

In the present research, the effect of three independent parameters including time (A), the mass ratio of hydrogen peroxide to chlorophenol (B), and catalyst (C) on the removal of chlorophenol (%) as the response by full factorial design of experiment was investigated. Each factor was explored in three levels. The pH was fixed at 6 in all runs. Table 2 demonstrates the matrix of experiment factors and their values.

The following model (Eq. 5) is fitted to the response variable (Y) in the form of a polynomial equation:

$$Y = \beta_0 + \sum_{j=1}^k \beta_j X_j + \sum_{i=1}^k \sum_{i < j} \beta_{ij} X_i X_j + \sum_{j=1}^k \beta_{jj} X_j^2 + \epsilon \quad (5)$$

where Y and k represent the response value, the number of independent factors, β_0 is constant-coefficient, $X_1 \dots X_k$ is coded independent factors, β_j is the coefficient of the first-order or linear influence, β_{jj} is the coefficient of quadratic or squared influence, and β_{ij} is representing the coefficient of interactions influence and ϵ is the random error responsible for any discrepancy or uncertainty between anticipated and

Table 2 Level and ranges of each factor

Factors	Code	Level and ranges		
		-1(Low)	0 (Middle)	+1(High)
Time (min)	A	10	20	30
Mass ratio of $\text{H}_2\text{O}_2/\text{CP}$ (%)	B	2.0	4	6
Catalyst (gr L^{-1})	C	1.5	3	4.5

actual value. Considering the three independent variables in this work, the regression equation for the second-order quadratic model is given as the following (Eq. 6):

$$Y = \beta_0 + \beta_1x_1 + \beta_2x_2 + \beta_3x_3 + \beta_{11}x_1^2 + \beta_{22}x_2^2 + \beta_{33}x_3^2 + \beta_{12}x_1x_2 + \beta_{13}x_1x_3 + \beta_{23}x_2x_3 \quad (6)$$

The general model for three-level full factorial design is given by 3^k in which k represents the number of design variables. Hence, in this study for the three aforementioned independent variables, there would be 27 experimental runs. Table 3 demonstrates design points, including three main variables and actual and predicted values of the response values. For conducting experimental design and statistical interpretations of the results besides determining the coefficients of the regression model (Eq. 6), the Design-Expert software version 13 was utilized.

Results and discussion

The ANOVA tests and statistical analysis

In this research, to achieve the optimal conditions, the effect of three independent parameters on the response was evaluated by full factorial design. The mean squares, the sum of squares, F value, and P values of each variable are demonstrated in Table 4. Based on the results of the ANOVA, the F-value of 431.1 indicates that the regression model is significant. In other words, it implies that there is a 0.01% chance that this F-value could happen because of the noise. Based on the statistical criteria and as recommended by Design-Expert software, the parameters that have P values equal to or less than 0.05 are considered significant. According to Table 4, A, B, C, AB, AC, A^2 , B^2 , and C^2 are significant model terms as they have P values less than 0.05. To determine the most proper transformation of the response values, the diagnostic Box-Cox is utilized. In this study, based on the results of the Box-Cox plot, the square root

Table 3 Full Factorial Design results of three independent variables and CP removal (%)

Run No	Time (min)	Mass ratio of H ₂ O ₂ to CP (%)	Catalyst (g/l)	Actual value	Predicted value
1	20	4	3	54	54.3
2	10	2	4.5	18	17.97
3	20	2	4.5	49	47.61
4	30	4	4.5	98.5	95.06
5	30	2	3	66.1	69.55
6	20	4	1.5	40.7	43.95
7	20	2	3	46	42.90
8	10	6	4.5	21	21.16
9	30	6	3	92	86.86
10	20	6	1.5	44.2	43.03
11	10	4	1.5	18	17.22
12	10	4	3	23	22.37
13	20	6	4.5	56	56.85
14	10	6	3	20	20.07
15	20	4	4.5	58.3	59.13
16	20	6	3	50	52.70
17	30	6	1.5	70	71.74
18	10	4	4.5	24.5	23.91
19	30	4	3	87	86.49
20	30	6	4.5	94	95.25
21	10	2	1.5	11	11.69
22	30	2	4.5	76	78.32
23	10	6	1.5	16	15.44
24	20	2	1.5	35	33.29
25	30	2	1.5	57	54.90
26	30	4	1.5	69.5	70.72
27	10	2	3	15	16.32

Table 4 ANOVA results for the removal of chlorophenol using the heterogeneous Fenton process

Response: Removal of CP			Transform: Square root			Constant: 0
Source	Sum of squares	DF	Mean square	F-value	<i>p</i> value	Percent contribution (%)
Model	104.27	9	11.59	431.10	<0.0001	Significant
A-Time	94.14	1	94.14	3503.03	<0.0001	90.28
B-H ₂ O ₂ /CP	2.26	1	2.26	84.21	<0.0001	2.17
C-Catalyst	4.99	1	4.99	185.59	<0.0001	4.78
AB	0.2223	1	0.2223	8.27	0.0105	0.21
AC	0.2911	1	0.2911	10.83	0.0043	0.28
BC	0.0155	1	0.0155	0.5775	0.4577	0.015
A ²	0.7618	1	0.7618	28.35	<0.0001	0.73
B ²	1.32	1	1.32	49.10	<0.0001	1.27
C ²	0.2669	1	0.2669	9.93	0.0058	0.26
Residual	0.4569	17	0.0269			
Corrected Total	104.73	26				
Model Summary						
R ²	0.9956		Standard Dev	0.1639		
Adjusted R ²	0.9933		Mean	6.68		
Predicted R ²	0.9895		C.V %	2.45		
Adequate Precision	63.6491					

(λ = 0.5) transformation was recommended by the software to enhance the overall status of the experimental design.

The correlation between factors and the CP removal (%) in terms of coded factors are presented in Eqs. 7:

$$\begin{aligned} \text{Sqrt (Removal of CP (\%))} &= +7.37 + 2.29 A + 0.3546 B + 0.5264 C \\ &+ 0.1361 AB + 0.1558 AC - 0.0360 BC \\ &- 0.3563 A^2 - 0.4690 B^2 - 0.2109 C^2 \end{aligned} \tag{7}$$

To anticipate response values for particular levels of each parameter, the coded equation can be utilized. The low and high levels of each variable are coded by -1 and +1, respectively. By comparing each variable coefficient, their relevant effect on the response can be recognized. Moreover, by using the original units of each parameter for their given level in the actual equation, the anticipation of response values can be performed. Since coefficients are scaled to adapt the units of each variable, the actual equation cannot be utilized to ascertain their effect on the response (Hinkelmann 2012). As can be evident from the coefficient of variables in the coded equation, time is the most influential parameter in the removal of chlorophenol. The coefficient of determination or R-squared (R²) is explained as the amount of variation in the data elucidated by the ANOVA model (Hinkelmann 2012). In other words, R-squared is a kind of statistical estimation of how close the experimental data are to the fitted

regression line. R-squared is calculated based on the following equation (Eq. 8):

$$R^2 = \frac{SS_{\text{Model}}}{SS_{\text{Total}}} = \frac{104.27}{104.73} = 0.9956 \tag{8}$$

As a result, the model explains around 99% of the variability in the experiment, and just 1% of the total variability is not estimated by the perfect regression. It is obvious that 0 ≤ R² ≤ 1 and larger values of R-squared are more desirable. The adjusted-R² is a deviation of the R-squared statistics that reflect the number of model variables. It can be a beneficial tool for highly complicated experimental settings with dissimilar design parameters when one wants to evaluate the effect of variation in the number of model terms (Hinkelmann 2012). The predicted R² and adjusted R² are 0.9895 and 0.9933, respectively, which indicates reasonable harmony between them because the difference between them is less than 0.2.

Moreover, based on Fig. 5a, as the actual and predicted outcomes are adequately close together and have enough harmony, the precision and correctness of the regression model are confirmed. The normal probability plot indicates whether the residuals track the straight line and normal distribution or not. As is evident from Fig. 5b, the experimental data are distributed evenly on a straight line.

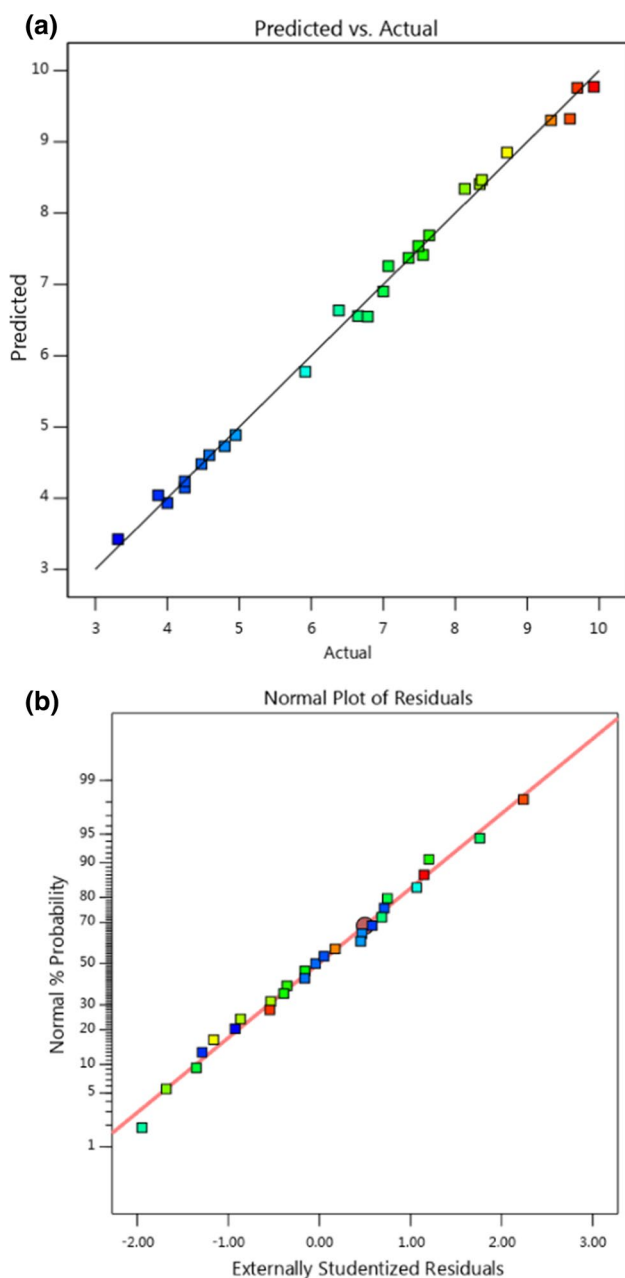


Fig. 5 **a** Comparison between anticipated and experimental quantities for the removal of the CP in the heterogeneous Fenton process, **b** Normal probability diagram for the model

To establish the linear, quadratic, and interaction contribution of each parameter in the experiment, the percent of contribution is measured by the following equation (Eq. 9):

$$\text{Percent of Contribution(\%)} = \frac{\text{the sum of squares of a factor}(SS_F)}{\text{the sum of squares of all factors}(SS_T)} \quad (9)$$

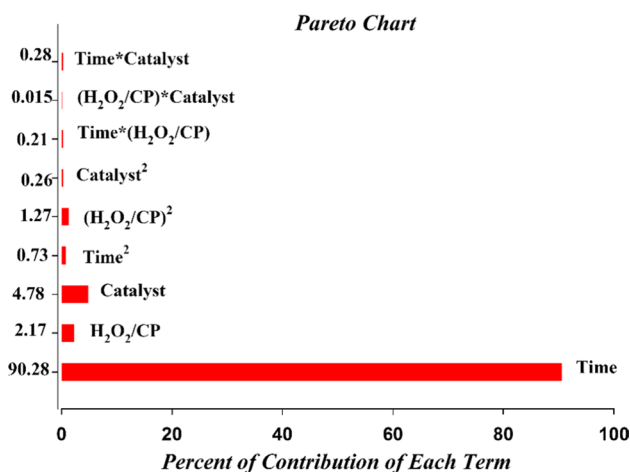


Fig. 6 Graphical Pareto chart for chlorophenol removal

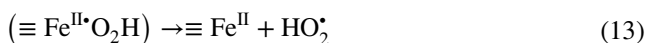
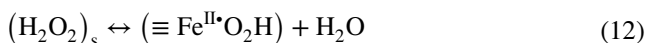
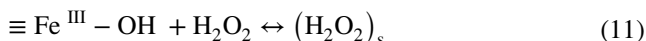
It was clear from Fig. 6 that the graphical Pareto study is performed to show the effect of each operative variable on the response and evaluated by the subsequent equation (Eq. 10).

$$P_i = \left(\frac{b_i^2}{\sum b_i^2} \right) \times 100 \quad (10)$$

The term b_i signifies the effect of the numerical coefficient for each variable. The time and concentration of catalyst were the imperative influences that affect the removal of CP.

Mechanism of heterogeneous Fenton process

Typically, due to the simplicity of recovery, significant catalytic activity, low toxicity, and cost-effectiveness of iron-based materials, they are regarded as excellent heterogeneous Fenton catalysts (Thomas et al. 2021). Iron leaching from the solid catalyst and heterogeneous catalytic mechanism are two methods by which hydroxyl radicals are produced in the heterogeneous Fenton reactions (He et al. 2016). By investigating the reactions of hydroxyl radicals on the solid Fe₂O₃ supported on silica catalyst, the mechanism of heterogeneous catalytic degradation of hydrogen peroxide can occur as the following (Eqs. 11–13):



In the above equations, $\equiv \text{Fe}^{\text{III}}$ demonstrates the iron existing on the surface of $\text{Fe}_2\text{O}_3/\text{SiO}_2$. The incorporation of hydrogen peroxide at the surface of $\equiv \text{Fe}^{\text{III}} - \text{OH}$ generates the solid complex hydrogen peroxide (Eq. 11). After that, the generation of a transition state complex ($\equiv \text{Fe}^{\text{II}}\text{O}_2\text{H}$) was occurred by a ligand to metal charge transformation (Eq. 12). Then, the complex dissociates and generates HO_2^\bullet (Eq. 13), and subsequently, hydroxyl radical is produced in the presence of $\equiv \text{Fe}^{\text{II}}$ and hydrogen peroxide (Eq. 14). This mechanism demonstrates the recycling of ferric ions and ferrous ions on the surface, as a result, $\equiv \text{Fe}^{\text{III}} - \text{OH}$ is considered as a heterogeneous catalyst. Regardless of the pure heterogeneous Fenton reaction, by the homogeneous Fenton process, the iron extract from the solid catalyst improved the reaction speed (Wang et al. 2010; Hartmann et al. 2010).

A schematic of the treatment of CP by $\alpha\text{-Fe}_2\text{O}_3/\text{SiO}_2$ as a heterogeneous Fenton catalyst is presented in Fig. 7. As mentioned before, at first, the pollutants were enriched to round the $\alpha\text{-Fe}_2\text{O}_3/\text{SiO}_2$. At that point, the H_2O_2 reacted with the Fe^{2+} on the surface of the catalyst. Therefore, hydroxyl radicals were produced and the oxidation of Fe^{2+} to Fe^{3+} occurred. In this condition, the CP was condensed at the surface of catalyst support and attacked by the generated hydroxyl radicals. After that, the degraded CP was desorbed, and the catalyst will be able to condense the CP again. Finally, a high degradation of CP occurred.

Effect of operational variables on the removal of chlorophenol

Among all influential factors in the heterogeneous Fenton process, always the pH has a substantial influence, since

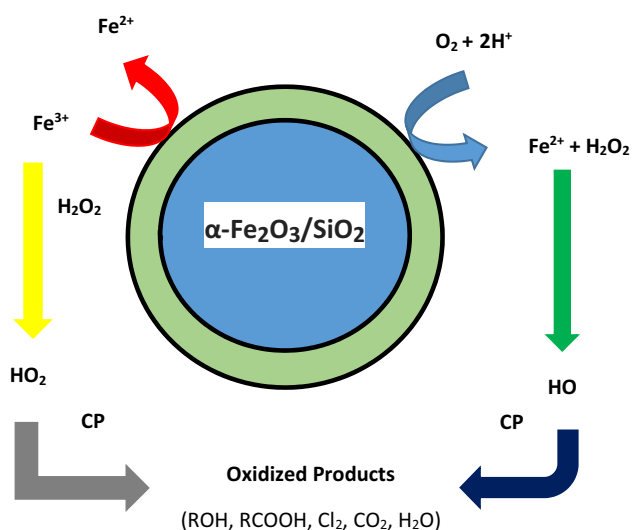


Fig. 7 A schematic diagram of the treatment of CP by $\alpha\text{-Fe}_2\text{O}_3/\text{SiO}_2$ as a heterogeneous Fenton catalyst

it significantly distresses the leaching of iron ions. Thus, the influence of pH on the removal of CP was investigated at first. It is well known that the optimum pH in the classical Fenton method is around 3.0, but in this process, before experimental design and in preliminary tests, a wider initial pH range of 3 to 9.0 was investigated for degradation of CP. The efficiency of the process was very low in alkaline pH, due to the precipitation of the leached Ferrous as $\text{Fe}(\text{OH})_3$. In neutral and acid conditions, the process efficiency was better in acidic media. The real pH of synthetic wastewater containing CP was around 6, and in this pH, the efficiency was a little better than other acidic pHs. Therefore, the pH of 6 was chosen in all runs since the comfort of operation was fixed and not investigated as a variable in the design of the experiment. The increase in CP degradation at lower pH could be originated from the faster dissolution of iron from $\alpha\text{-Fe}_2\text{O}_3/\text{SiO}_2$, which was favorable for producing hydroxyl radicals by activating H_2O_2 .

Influence of time

To inspect the effects of operational factors on the removal of chlorophenol, three dimension and counterplots were utilized. It is evident that in these plots, the effects of two parameters are explored, whereas the other factors are held constant. As it can be obvious from Fig. 8a, b, with an increase in the reaction time, the removal of chlorophenol will increase. In other words, increasing time from 10 to 20 min increases the chlorophenol degradation and this trend is continuous from 20 to 30 min, too. At the highest values of time, chlorophenol degradation reaches around 97%. Because with passing time, more pollutant molecules were adsorbed on the catalyst surface gradually and more Fe^{2+} were oxidized to Fe^{3+} , and subsequently, more H_2O_2 is decomposed to the hydroxyl radicals which effectively degrade chlorophenol molecules. These results are in agreement with Hassani et al. and Shokri (Hassani et al. 2016; Shokri 2018).

Influence of $\text{H}_2\text{O}_2/\text{CP}$ mass ratio

It is evident from Fig. 9a, b, that increasing the mass ratio of H_2O_2 to chlorophenol increases chlorophenol degradation. The reason is due to the H_2O_2 being the precursor of OH^\bullet hence removal will be increased with increasing the concentration of hydrogen peroxide to chlorophenol. However, this tendency is more obvious and stronger when the mass ratio of hydrogen peroxide to chlorophenol increases from its lowest value, 2 to 4, and after that, the rate of chlorophenol removal will not be remarkable until 5, and after that, from 5 to 6, chlorophenol removal will even decrease gradually. Further increase in the concentration of H_2O_2 influenced the reaction of generated OH^\bullet with extra hydrogen peroxide molecules to generate HO_2^\bullet



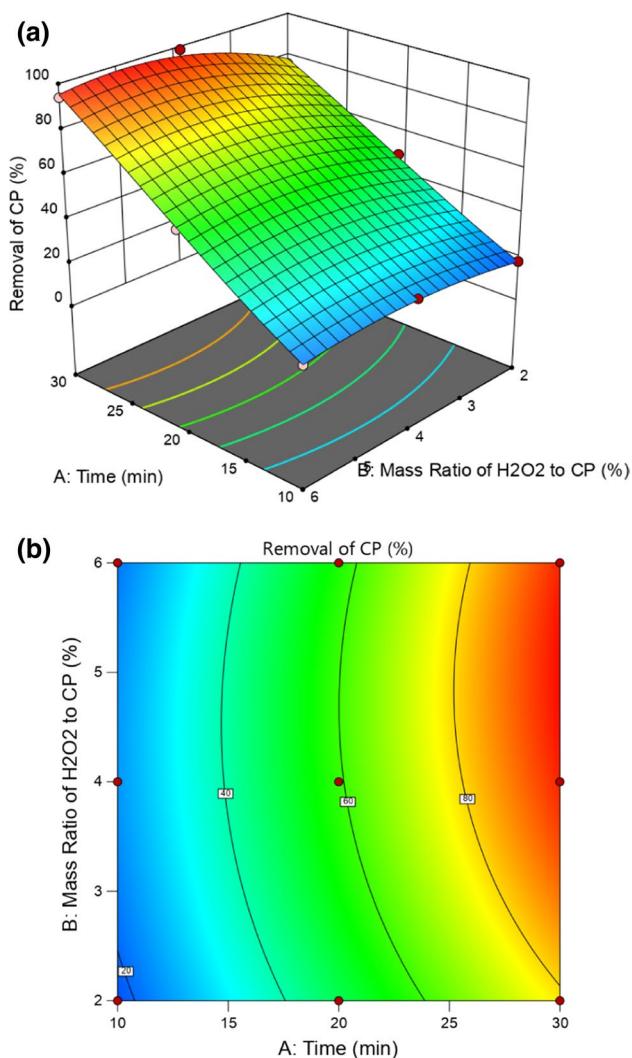
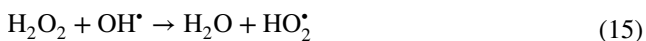


Fig. 8 **a** The 3D, and **b** counterplots of time and mass ratio of $\text{H}_2\text{O}_2/\text{CP}$ at catalyst dosage of 4.5 mg.L^{-1}

which has a lower oxidizing capability based on the following reaction (Eq. 15):



The H_2O_2 performs as a free radical scavenger at higher concentrations, as a result, the removal of chlorophenol was reduced at a great concentration of H_2O_2 to chlorophenol according to the following equation (Eq. 16):



Moreover, the auto-degradation of hydrogen peroxide to water and O_2 and the reaction of hydrogen peroxide with OH^\bullet instead of chlorophenol molecules have occurred. These results are in agreement with the investigation of Shokri (Shokri 2018).

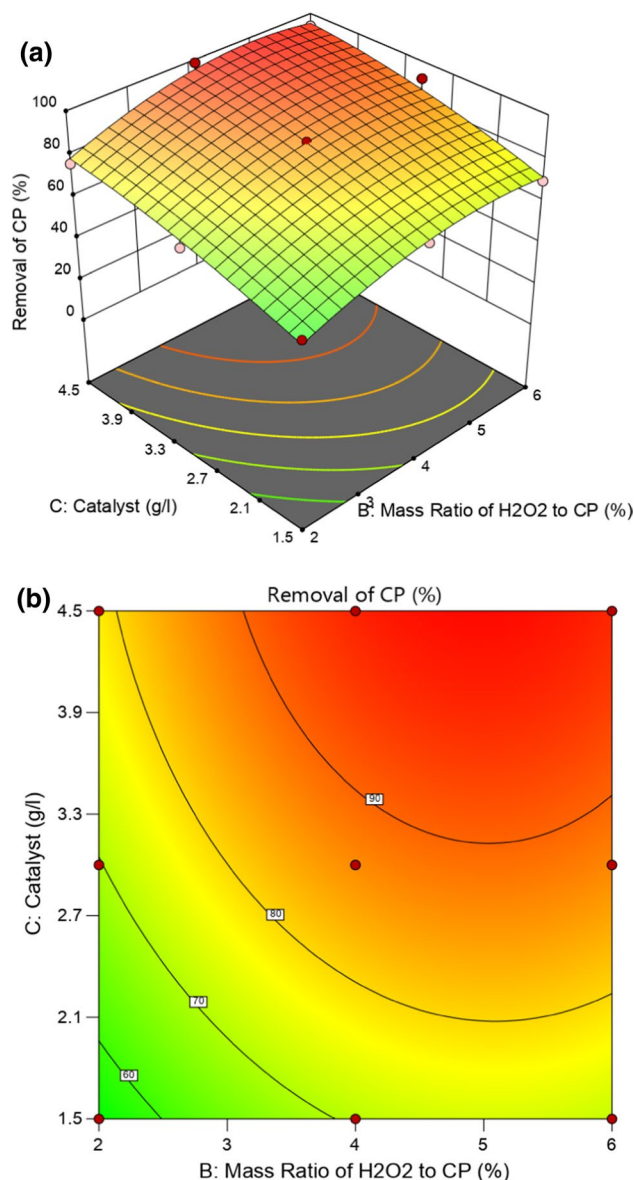


Fig. 9 The 3D **(a)**, and counterplots **(b)**, of mass ratio of $\text{H}_2\text{O}_2/\text{CP}$ and catalyst dosage at the time of 30 min

Influence of catalyst dosage

It is quite obvious from Fig. 10a, b that always an increase in the $\alpha\text{-Fe}_2\text{O}_3/\text{SiO}_2$ as catalyst results in enhancement in the removal of chlorophenol. However, after the value of almost 3.5 gr/l , the removal performance of catalyst is not quite notable and removal of chlorophenol changes with low speed or even less removal obtained. This trend can be elucidated that increasing the catalyst dosage leads to a higher generation of ferrous ions which can react with hydrogen peroxide and decompose them to more non-selective powerful hydroxyl radicals for degradation of chlorophenol molecules. However, at higher levels of catalyst, the number of



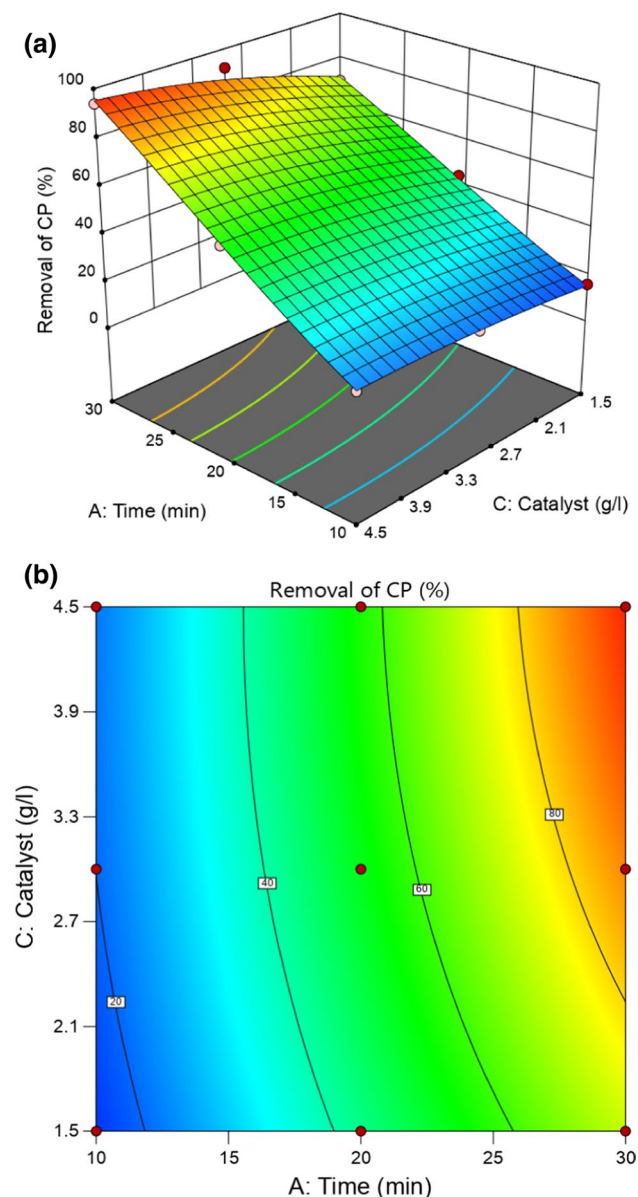


Fig. 10 **a** The 3D, and **b** counterplots of time and catalyst at a mass ratio of $\text{H}_2\text{O}_2/\text{CP}$ of 6

its active sites is lower and hence shows slow degrees of removal effect or even low. This result is in harmony with Hassani et al. 2016.

The increase in the concentration of $\alpha\text{-Fe}_2\text{O}_3/\text{SiO}_2$ can increase the number of reaction sites for obliging hydroxyl radicals and contaminants in wastewater donated to the increase in the removal of CP. The enthalpy and entropy of the adsorbed pollutant molecules onto the active sites were decreased, and therefore, the oxidation of intermediate molecules into stable termination products such as Cl_2 , and CO_2 happened easily. These results are in agreement with the finding of Gupta et al. 2009a.

Response optimization and confirmation

Process optimization was conducted according to the full factorial model using the desirability function. In any case, to make optimization easy, the trick is to combine all the goals into one objective function. The best solution is the application of desirability as the overall measure of success when optimizing multiple responses. To determine the best combination of responses, an objective function, $D(x)$, was utilized which involves the application of a multiplicative rather than an additive meaning. Statisticians call this the geometric mean. For overall and individual desirability, the equations are as the following (Eqs. 17–18):

$$\text{Desirability } (D) = (d_1 \times d_2 \times \dots \times d_n)^{1/n} = \left(\prod_{i=1}^n d_i \right)^{1/n} \quad (17)$$

$$d_i = \frac{\text{Optimum value of response} - \text{lower limit of response}}{\text{Upper limit of response} - \text{lower limit of response}} \quad (18)$$

The d_i , which ranges from 0 to 1 (least to most desirable, respectively), indicates the desirability of each factor (i) response, and n is the number of responses being optimized. Convert all criteria into one scale of desirability (small d 's) so that they can be combined into one, easily optimized value, the big D . By condensing all responses into one overall desirability, none of them need to be favored more than any other. Hence, the goals of operational factors and response were set in range and at maximum, respectively (the lower limit was set at 80 and the upper limit was set at 100). The optimized results are presented in Table 5.

Kinetic study

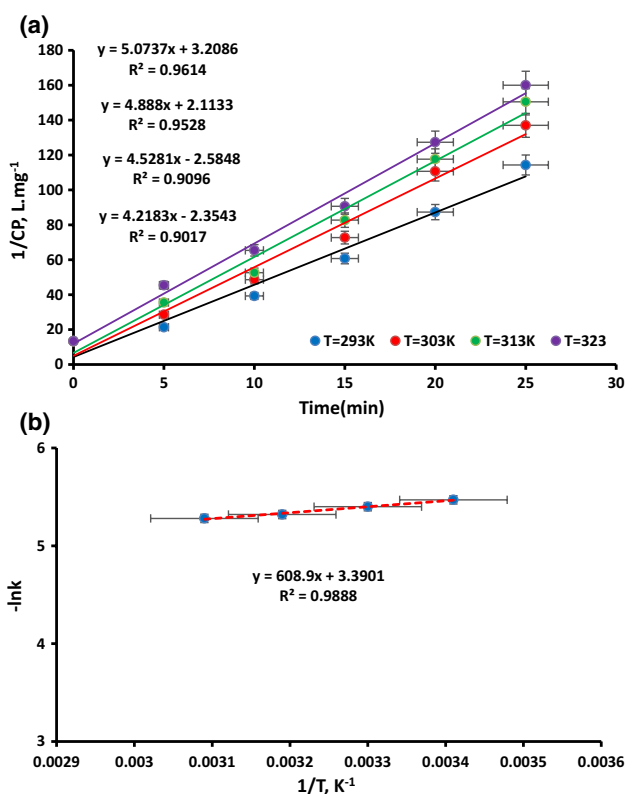
The kinetic study was performed by relating the removal of chlorophenol as a function of time, using the heterogeneous Fenton reaction. As it is evident from Fig. 11 a, the results demonstrated a well-fitted second-order reaction. According to the results of the kinetic model, the concentration of OH^\bullet is the only significant parameter for the determination of reaction rate. The 0.00421, 0.00452, 0.00488, and 0.00507 ($\text{L mg}^{-1} \text{min}^{-1}$) are the rate constant values at temperatures of 293, 303, 313, and 323 K, respectively (Körbahti 2007). Figure 11a demonstrates the heterogeneous Fenton reaction well fitted with a second-order rate equation, followed by the mathematical expression (Eq. 19);

$$\frac{1}{[\text{CP}]_t} = \frac{1}{[\text{CP}]_0} + kt \quad (19)$$



Table 5 Optimal operational conditions for maximum removal of CP (%)

Variables	Optimum values for the removal of CP (%)
Time	30
The mass ratio of H ₂ O ₂ /CP	4.96
Catalyst dosage	4.5
Removal of CP (%)	Prediction (97.71), Experimental (98.9)
Desirability	0.890

**Fig. 11** **a** Determining the order and kinetic rate constant, **b** E_a values for heterogeneous Fenton oxidations

where k is the rate constant (L mg⁻¹ min⁻¹), t is time (min), $[CP]_t$ is the concentration of 4-Chlorophenol at a time “ t ” and $[CP]_0$ is the concentration of 4-Chlorophenol at time $t=0$.

This indicates that the number of active sites available in $\alpha\text{-Fe}_2\text{O}_3/\text{SiO}_2$ and the concentration of OH^\bullet are the main determinants of the degree of heterogeneous Fenton reaction of organics in wastewater. At various levels of temperature, the rate constants for the oxidation of wastewater were ascertained

and utilized for the calculation of the activation energy using the Arrhenius equation. Then, the activation energy (E_a) is measured from Fig. 11b at 5.05 kJ/mol.

Thermodynamic studies

By application of the classical Van't Hoff equation for the heterogeneous Fenton reactions, the thermodynamic factors including a variation in entropy (ΔS), variation in enthalpy (ΔH), and variation in Gibbs free energy (ΔG) were measured. The increased spontaneity of the reaction, such as a tendency to enter into a solution, was indicated by the positive value of ΔS . In order to diagnose the nature of the reaction, either exothermic or endothermic, ΔH is utilized (Gupta et al. 2009b, a). The negative sign of ΔG implies the randomness of the oxidation reaction. The variations in enthalpy and entropy are relevant to the equilibrium constant by the resulting expression (Eq. 20):

$$\ln K_e = \frac{\Delta S}{R} - \frac{\Delta H}{RT} \quad (20)$$

where the ΔS and ΔH values were attained from the intercept and slope of the plot ($\ln K_e$ vs. $1/T$) and K_e is the reaction equilibrium constant (Gupta et al. 2011b, a). Table 6 demonstrates the thermodynamic factors. The positive value of ΔS implies spontaneity at the solid-solution interface. The positive value of ΔH implies that the oxidation reaction was inherently endothermic and it might be considered chemical oxidation. Moreover, the variation in reaction ΔG was highly correlated with values of ΔH and ΔS as presented in the following equation (Eq. 21):

$$\Delta G = \Delta H - T\Delta S \quad (21)$$

For heterogeneous Fenton reactions, the ΔS and ΔH values were 35.13 J/mol K and 5.95 kJ/mol, respectively. These values indicate that $\alpha\text{-Fe}_2\text{O}_3/\text{SiO}_2$ has reduced the ΔH value in heterogeneous Fenton oxidation. The low ΔS value of the heterogeneous Fenton reaction can be attributed to the surface condensation of molecules; as a result, the ΔH value was reduced, too. The presence of active energy sites in $\alpha\text{-Fe}_2\text{O}_3/\text{SiO}_2$ can be the reason for the reduction in of

Table 6 Thermodynamic characteristics of heterogeneous Fenton (with $\alpha\text{-Fe}_2\text{O}_3/\text{SiO}_2$) in the removal of CP

Heterogeneous Fenton oxidation				
S. No	Temperature(K)	ΔG (kJ/mol)	ΔH (kJ/mol)	ΔS (J/molK)
1	293	-4.343	5.95	35.13
2	303	-4.694		
3	313	-5.045		
4	323	-5.396		

ΔH value. The presence of active energy sites can be proved from the presence of free electrons in catalysts determined by ESR spectroscopy which results from the cleavage of C–C bonds in the network structure of the carbon matrix (Karthikeyan et al. 2011). The generation of OH^\bullet and sustainable reaction can be feasible only when the electron was abstracted from the hydroxides produced due to the Fenton reaction.

Conclusion

In this research, the FFD design was employed to investigate the removal of chlorophenol in synthetic wastewater by $\alpha\text{-Fe}_2\text{O}_3/\text{SiO}_2$ as a synthesized catalyst in heterogeneous Fenton reactions. The synthesized $\alpha\text{-Fe}_2\text{O}_3/\text{SiO}_2$ was characterized by the SEM, FTIR, and XRD methods. The influence of three critical factors including time, the mass ratio of H_2O_2 to chlorophenol, and the amount of catalyst on the removal of CP has been studied. The optimal conditions anticipated by the fitted model were as the following: time = 30 min, the mass ratio of H_2O_2 to chlorophenol = 4.96, and catalyst dosage = 4.5 gr L^{-1} . The maximum efficiency in the experimental and predicted CP removal were 98.9 and 97.71%, respectively. The ANOVA results demonstrated an acceptable pseudo-second-order reaction kinetic model for the removal of CP. The high determination coefficient quantities ($R^2 = 0.9956$, Predicted $R^2 = 0.9895$, and Adjusted $R^2 = 0.9933$) validated the reliability of the model. To interpret the effect of each parameter besides their interactions on each other, the counter and the three-dimensional plots were used. The mechanism of catalyst in the degradation of CP was described. The kinetic study indicated that the degradation of CP followed a second-order model with rate constants in the range of $0.00421\text{--}0.00507 \text{ (L mg}^{-1} \text{ min}^{-1})$. The thermodynamic and kinetic parameters including ΔH° , ΔG° , E_a , and ΔS° were achieved in the range of 5.95 kJ mol^{-1} , -4.343 to $-5.396 \text{ kJ mol}^{-1}$, 5.05 kJ mol^{-1} , and $35.13 \text{ J mol}^{-1} \text{ K}^{-1}$, respectively. The thermodynamic studies showed that the treatment process is highly endothermic and spontaneous. The results showed that the heterogeneous Fenton using $\alpha\text{-Fe}_2\text{O}_3/\text{SiO}_2$ catalyst is a promising and effective solution for the removal of chlorophenol.

Declarations

Conflict of interest The authors declare that they have no known competing financial interests or personal relationships that could have appeared to influence the work reported in this paper.

References

- Barka N, Assabbane A (2008) Photocatalytic degradation of methyl orange with immobilized TiO_2 nanoparticles: effect of pH and some inorganic anions. *Phys Chem* 41:85–88
- Bharathi S, Nataraj D, Mangalaraj D et al (2010) Highly mesoporous $\alpha\text{-Fe}_2\text{O}_3$ nanostructures: preparation, characterization and improved photocatalytic performance towards Rhodamine B (RhB). *J Phys D Appl Phys* 43:015501. <https://doi.org/10.1088/0022-3727/43/1/015501>
- Chen D, Chen S, Jiang Y et al (2017) Heterogeneous Fenton-like catalysis of Fe-MOF derived magnetic carbon nanocomposites for degradation of 4-nitrophenol. *RSC Adv* 7:49024–49030. <https://doi.org/10.1039/c7ra09234b>
- Clematis D, Panizza M (2021) Electrochemical oxidation of organic pollutants in low conductive solutions. *Curr Opin Electrochem* 26:100665. <https://doi.org/10.1016/j.coelec.2020.100665>
- Feng Y, Han K, Jiang T et al (2019) Self-powered electrochemical system by combining Fenton reaction and active chlorine generation for organic contaminant treatment. *Nano Res* 12:2729–2735. <https://doi.org/10.1007/s12274-019-2506-5>
- Gonzalez-Olmos R, Kopinke FD, Mackenzie K, Georgi A (2013) Hydrophobic Fe-zeolites for removal of MTBE from water by combination of adsorption and oxidation. *Environ Sci Technol* 47:2353–2360. <https://doi.org/10.1021/es303885y>
- Gupta VK, Carrott PJM, Ribeiro Carrott MML, Suhas (2009a) Low-cost adsorbents: growing approach to wastewater treatment review. *Crit Rev Environ Sci Technol* 39:783–842. <https://doi.org/10.1080/10643380801977610>
- Gupta VK, Mittal A, Malviya A, Mittal J (2009b) Adsorption of carmoisine A from wastewater using waste materials-Bottom ash and deoiled soya. *J Colloid Interface Sci* 335:24–33. <https://doi.org/10.1016/j.jcis.2009.03.056>
- Gupta VK, Gupta B, Rastogi A et al (2011a) A comparative investigation on adsorption performances of mesoporous activated carbon prepared from waste rubber tire and activated carbon for a hazardous azo dye-Acid Blue 113. *J Hazard Mater* 186:891–901. <https://doi.org/10.1016/j.jhazmat.2010.11.091>
- Gupta VK, Jain R, Saleh TA et al (2011b) Equilibrium and Thermodynamic studies on the removal and recovery of Safranin-T dye from industrial effluents. *Sep Sci Technol* 46:839–846. <https://doi.org/10.1080/01496395.2010.535591>
- Hadi S, Taheri E, Amin MM et al (2020) Synergistic degradation of 4-chlorophenol by persulfate and oxalic acid mixture with heterogeneous Fenton like system for wastewater treatment: Adaptive neuro-fuzzy inference systems modeling. *J Environ Manage* 268:110678. <https://doi.org/10.1016/j.jenvman.2020.110678>
- Hartmann M, Kullmann S, Keller H (2010) Wastewater treatment with heterogeneous Fenton-type catalysts based on porous materials. *J Mater Chem* 20:9002–9017. <https://doi.org/10.1039/c0jm00577k>
- Hassani G, Takdastan A, Ghaedi M et al (2016) Optimization of 4-chlorophenol oxidation by manganese ferrite nanocatalyst with response surface methodology. *Int J Electrochem Sci* 11:8471–8485
- He J, Yang X, Men B, Wang D (2016) Interfacial mechanisms of heterogeneous Fenton reactions catalyzed by iron-based materials: a review. *J Environ Sci (china)* 39:97–109. <https://doi.org/10.1016/j.jes.2015.12.003>
- He J, Miller CJ, Collins R et al (2020) Production of a surface-localized oxidant during oxygenation of Mackinawite (FeS). *Environ Sci Technol* 54:1167–1176. <https://doi.org/10.1021/acs.est.9b03975>
- Hinkelmann K (2012) Design and analysis of experiments. *Des Anal Exp* 3:1–566. <https://doi.org/10.1002/9781118147634>
- Hou H, Zeng X, Zhang X (2020) 2D/2D heterostructured photocatalyst: rational design for energy and environmental applications.



- Sci China Mater 63:2119–2152. <https://doi.org/10.1007/s40843-019-1256-0>
- Karimi A, Aghbolaghy M, Khataee A, Shoa Bargh S (2012) Use of enzymatic bio-fenton as a new approach in decolorization of malachite green. *Sci World J*. <https://doi.org/10.1100/2012/691569>
- Karthikeyan S, Titus A, Gnanamani A et al (2011) Treatment of textile wastewater by homogeneous and heterogeneous Fenton oxidation processes. *Desalination* 281:438–445. <https://doi.org/10.1016/j.desal.2011.08.019>
- Körbahti BK (2007) Response surface optimization of electrochemical treatment of textile dye wastewater. *J Hazard Mater* 145:277–286. <https://doi.org/10.1016/j.jhazmat.2006.11.031>
- Li Q, Chen Z, Wang H et al (2021a) Removal of organic compounds by nanoscale zero-valent iron and its composites. *Sci Total Environ* 792:148546. <https://doi.org/10.1016/j.scitotenv.2021.148546>
- Li Q, Gao X, Liu Y et al (2021b) Biochar and GAC intensify anaerobic phenol degradation via distinctive adsorption and conductive properties. *J Hazard Mater* 405:124183. <https://doi.org/10.1016/j.jhazmat.2020.124183>
- Liang X, Zhong Y, He H et al (2012) The application of chromium substituted magnetite as heterogeneous Fenton catalyst for the degradation of aqueous cationic and anionic dyes. *Chem Eng J* 191:177–184. <https://doi.org/10.1016/j.cej.2012.03.001>
- Metafonova G, Philippova N, Batoev V (2011) The effect of wavelength and pH on the direct photolysis of chlorophenols by ultraviolet excilamps. *Eng Lett* 19(1):20–23
- Morshed MN, Behary N, Bouazizi N et al (2020) Modification of fibrous membrane for organic and pathogenic contaminants removal: from design to application. *RSC Adv* 10:13155–13173. <https://doi.org/10.1039/d0ra01362e>
- Mushtaq F, Chen X, Torlakcik H et al (2020) Enhanced catalytic degradation of organic pollutants by multi-stimuli activated multiferoic nanoarchitectures. *Nano Res* 13:2183–2191. <https://doi.org/10.1007/s12274-020-2829-2>
- Nidheesh PV (2015) Heterogeneous Fenton catalysts for the abatement of organic pollutants from aqueous solution: a review. *RSC Adv* 5:40552–40577. <https://doi.org/10.1039/c5ra02023a>
- Nidheesh PV, Gandhimathi R, Ramesh ST (2013) Degradation of dyes from aqueous solution by Fenton processes: a review. *Environ Sci Pollut Res* 20:2099–2132. <https://doi.org/10.1007/s11356-012-1385-z>
- Nikazar M, Gholivand K, Mahanpoor K (2008) Photocatalytic degradation of azo dye acid red 114 in water with TiO₂ supported on clinoptilolite as a catalyst. *Desalination* 219:293–300. <https://doi.org/10.1016/j.desal.2007.02.035>
- Pervez MN, Telegin FY, Cai Y et al (2019) Efficient degradation of mordant blue 9 using the fenton-activated persulfate system. *Water (switzerland)* 11:2532. <https://doi.org/10.3390/w11122532>
- Pervez MN, He W, Zarra T et al (2020) New sustainable approach for the production of Fe₃O₄/Graphene oxide-activated persulfate system for dye removal in real wastewater. *Water (switzerland)* 12:733. <https://doi.org/10.3390/w12030733>
- Rauf MA, Ashraf SS (2009) Radiation induced degradation of dyes—an overview. *J Hazard Mater* 166:6–16. <https://doi.org/10.1016/j.jhazmat.2008.11.043>
- Rocha RP, Soares OSGP, Órfão JJM et al (2021) Heteroatom (N, S) Co-doped CNTs in the phenol oxidation by catalytic wet air oxidation. *Catalysts* 11:578. <https://doi.org/10.3390/catal11050578>
- Shokri A (2018) Application of Sono-photo-Fenton process for degradation of phenol derivatives in petrochemical wastewater using full factorial design of experiment. *Int J Ind Chem* 9:295–303. <https://doi.org/10.1007/s40090-018-0159-y>
- Shokri A (2020) Degradation of 4-Chloro phenol in aqueous media thru UV/Persulfate method by artificial neural network and full factorial design method. *Int J Environ Anal Chem*. <https://doi.org/10.1080/03067319.2020.1791328>
- Sun M, Chu C, Geng F et al (2018) Reinventing Fenton chemistry: iron oxychloride nanosheet for pH-insensitive H₂O₂ activation. *Environ Sci Technol Lett* 5:186–191. <https://doi.org/10.1021/acs.estlett.8b00065>
- Sun H, Xie G, He D, Zhang L (2020) Ascorbic acid promoted magnetite Fenton degradation ofalachlor: mechanistic insights and kinetic modeling. *Appl Catal B Environ* 267:118383. <https://doi.org/10.1016/j.apcatb.2019.118383>
- Thomas N, Dionysiou DD, Pillai SC (2021) Heterogeneous Fenton catalysts: a review of recent advances. *J Hazard Mater* 404:124082. <https://doi.org/10.1016/j.jhazmat.2020.124082>
- Waite TD, Chen Y, Miller CJ (2021) Heterogeneous Fenton chemistry revisited: mechanistic insights from ferrihydrite-mediated oxidation of formate and oxalate. *Environ Sci Technol* 55:14414–14425. <https://doi.org/10.1021/acs.est.1c00284>
- Wang W, Zhou M, Mao Q et al (2010) Novel NaY zeolite-supported nanoscale zero-valent iron as an efficient heterogeneous Fenton catalyst. *Catal Commun* 11:937–941. <https://doi.org/10.1016/j.catcom.2010.04.004>
- Xu L, Wang J (2012) Magnetic nanoscaled Fe₃O₄/CeO₂ composite as an efficient fenton-like heterogeneous catalyst for degradation of 4-chlorophenol. *Environ Sci Technol* 46:10145–10153. <https://doi.org/10.1021/es300303f>
- Ye Y, Yi W, Liu W et al (2020) Remarkable surface-enhanced Raman scattering of highly crystalline monolayer Ti₃C₂ nanosheets. *Sci China Mater* 63:794–805. <https://doi.org/10.1007/s40843-020-1283-8>
- Zhang N, Tsang EP, Chen J et al (2019) Critical role of oxygen vacancies in heterogeneous Fenton oxidation over ceria-based catalysts. *J Colloid Interface Sci* 558:163–172. <https://doi.org/10.1016/j.jcis.2019.09.079>

Springer Nature or its licensor holds exclusive rights to this article under a publishing agreement with the author(s) or other rightsholder(s); author self-archiving of the accepted manuscript version of this article is solely governed by the terms of such publishing agreement and applicable law.